arXiv:astro-ph/0001101v1 7 Jan 2000

CCD PHOTOMETRY OF THE GLOBULAR CLUSTER ω CENTAURI. I. METALLICITY OF RR LYRAE STARS FROM *Caby* PHOTOMETRY

Soo-Chang Rey[1], Young-Wook Lee, and Jong-Myung Joo[1]
Center for Space Astrophysics & Department of Astronomy,
Yonsei University, Shinchon 134, Seoul 120-749, Korea
Electronic mail : (screy, ywlee, jmjoo)@csa.yonsei.ac.kr

Alistair Walker
Cerro Tololo Inter-American Observatory, NOAO, Casilla 603, La Serena, Chile
Electronic mail : awalker@noao.edu

and

Scott Baird
Department of Physics & Astronomy,
Benedictine College, Atchison, Kansas 66002-1499,
and Department of Physics & Astronomy,
University of Kansas, Lawrence, Kansas 66045-2151, USA
Electronic mail : baird@kuphsx.phsx.ukans.edu

ABSTRACT

We present new measurements of the metallicity of 131 RR Lyrae stars in the globular cluster ω Centauri, using the hk index of the *Caby* photometric system. The hk method has distinct advantages over ΔS and other techniques in determining the metallicity of RR Lyrae stars, and has allowed us to obtain the most complete and homogeneous metallicity data to date for the RR Lyrae stars in this cluster. For RR Lyrae stars in common with the ΔS observations of Butler et al. (1978) and Gratton et al. (1986), we have found that our metallicities, $[Fe/H]_{hk}$, deviate systematically from their ΔS metallicity, while our $[Fe/H]_{hk}$ for well observed field RR*ab* stars are consistent with previous spectroscopic measurements. We conclude that this is due to the larger errors associated with the previous ΔS observations for this cluster. The M_V(RR) - [Fe/H] and period-shift - [Fe/H] relations obtained from our new data are consistent with the evolutionary models predicted by Lee (1991), confirming that the luminosity of RR Lyrae stars depends on evolutionary status as

[1]Visiting Astronomer, Cerro Tololo Inter-American Observatory, National Optical Astronomy Observatories, which is operated by the Association of Universities for Research in Astronomy, Inc. (AURA) under cooperative agreement with the National Science Foundation.

well as metallicity. Using the period - amplitude diagram, we have also identified highly evolved RR*ab* stars in the range of -1.9 $\leq$ [Fe/H] $<$ -1.5, as predicted from the synthetic horizontal-branch models.

Subject headings: globular clusters: individual (ω Centauri) — RR Lyrae variable — stars: abundances — stars: horizontal-branch

1. INTRODUCTION

For dating globular clusters and several other important problems (e.g., measuring distances to Population II objects), it is essential to know the luminosity of the RR Lyrae stars, M_{bol}(RR), and how it varies with metal abundance (see Sandage 1990b; Lee, Demarque, and Zinn 1990, hereafter LDZ). The variation of M_{bol}(RR) with [Fe/H] affects the age - metallicity relation of the Galactic globular cluster system, and thus provides constraints on the scenarios of the Galaxy formation. However, due to the variety of different techniques used, the particular data set chosen, and the reddening corrections adopted, there is no consensus on the size of the dependency of M_{bol}(RR) upon [Fe/H] (Layden et al. 1996). To investigate and resolve the problem of the dependence of M_{bol}(RR) on [Fe/H], one needs a large sample of RR Lyrae stars, spanning a wide range of [Fe/H], for which precise measurements of relative luminosity and [Fe/H] exist. The RR Lyrae stars in ω Cen are an ideal sample for this study. In ω Cen, there is a wide range in [Fe/H], and clearly the relative values of M_{bol}(RR) can be inferred straightforwardly from their mean apparent visual magnitudes since they are all located at the same distance and are all reddened by the same amount.

However, investigations by Freeman & Rodgers(1975), Butler et al. (1978, hereafter BDE), Sandage (1982), and Gratton et al. (1986, hereafter GTO) have revealed that the M_{bol}(RR) - [Fe/H] correlation in ω Cen is peculiar: a few metal-rich ([Fe/H] > -1.1) RR Lyrae stars in their sample are fainter than the more metal-poor ones, but no obvious correlation exists among the metal-poor ([Fe/H] < -1.4) RR Lyrae stars. This and the lack of a period-shift - [Fe/H] correlation amongst the variables was recognized by Sandage (1982) as a possible contradiction to his steep correlation between M_{bol}(RR) and [Fe/H]. In general these "discrepant" observational results were simply considered to be yet another anomaly of the stellar population of ω Cen (see also Smith 1995).

Recent advances in our understanding of the evolution of horizontal-branch (HB) stars are throwing new light on this long-standing problem. In particular, the HB evolutionary models by Lee (1990) suggest that M_{bol}(RR) depends on HB morphology as well as metallicity, especially when the HB morphology is extremely blue, due to the effect of redward evolution off the zero-age horizontal-branch (ZAHB). Using these model calculations, Lee (1991) has shown that the observed nonlinear behavior of M_{bol}(RR) with [Fe/H] in ω Cen is not something peculiar,

but is in fact predicted. The detailed model calculations suggest that two effects are responsible for the observed behavior of M_{bol}(RR) with [Fe/H] in ω Cen, and are: (1) the abrupt increase in M_{bol}(RR) near [Fe/H] = -1.5 as RR Lyrae stars become highly evolved stars from the blue side of the instability strip as HB morphology gets bluer with decreasing [Fe/H], and (2) the nonmonotonic behavior of the HB morphology with decreasing [Fe/H], which together with the first effect makes the correlation between M_{bol}(RR) and [Fe/H] looks like a step function, because M_{bol}(RR) depends sensitively on HB morphology. Despite the lack of a complete understanding of why HB morphology changes as it does, the definite conclusions from Lee's (1991) work are: (1) The correlation between M_{bol}(RR) and [Fe/H] in the halo of our Galaxy is probably not linear due to the effect of HB morphology (evolution). (2) The use of a simple linear relationship between M_{bol}(RR) and [Fe/H] in deriving the distances to blue HB clusters should be avoided. This suggests that when the distances to the population II objects are to be estimated using the RR Lyrae stars, the HB type of the stellar population, as well as metallicity, must be known.

Although the ω Cen data do appear to support this model, a definite conclusion was not possible because of the uncertainty in [Fe/H] and of the lack of metal-rich stars in the available data. In order to provide a more complete and homogeneous sample of RR Lyrae stars with relatively well-measured metallicity, we obtained [Fe/H] abundances for most of the RR Lyrae stars in ω Cen, using the *Caby* photometric system. The *Caby* photometric system is an expansion of the standard *uvby* system with the inclusion of a fifth filter, Ca, centered on the K and H lines of Ca II (90 $\AA$ FWHM). The hk index is defined as $hk = (Ca - b) - (b - y)$, and is found to be much more sensitive to metal abundance than the *Strömgren* m_1 index (Anthony-Twarog et al. 1991; Twarog & Anthony-Twarog 1991, 1995; Anthony-Twarog & Twarog 1998). The sensitivity of the hk index to metallicity changes is high at all [Fe/H] for hotter stars and also for cooler stars more metal-poor than [Fe/H] = -1.0. It is about three times more sensitive than the m_1 index (see Fig. 9 of Twarog & Anthony-Twarog 1995). Baird (1996, hereafter B96) extended *Caby* photometry to RR Lyrae stars of known metallicity and showed that the hk index retains good sensitivity even at the hottest phases of pulsation. It was demonstrated that isometallicity lines formed in the $hk/(b-y)$ diagram are single valued with respect to both $b-y$ and hk. Therefore, the $hk/(b-y)$ diagram gives consistent metallicities throughout a star's pulsational cycle, including during rising light and near maximum light, when ΔS results are unreliable, and so precise knowledge of light curve phase is unnecessary. An additional advantage of the photometric approach is that standard crowded-field techniques can be used to measure stars even in rich cluster centers.

In this paper we present the results of a new *Caby* photometric survey of 131 RR Lyrae stars in ω Cen, from which metal abundances are derived via the hk index. In section 2, we describe the observations and the reduction procedures. The adopted metallicity calibration procedures are outlined in section 3. In section 4, we present the results of our metallicity determination for field RR Lyrae stars and ω Cen RR Lyrae stars, with a comparison with the previous ΔS measurements. Finally, in section 5 we discuss the impact of our new metallicity measurements on the M_V(RR) - [Fe/H] and period-shift - [Fe/H] relations. The color-magnitude diagram resulting

from the *Caby* photometry, and a discussion of the metallicity distribution of giant branch stars will be presented in a future paper of this series.

2. OBSERVATIONS AND DATA REDUCTIONS

All the observations were made using the CTIO 0.9 m telescope and Tektronix 2048 No. 3 CCD during three nights of an observing run in March 1997. We covered ω Cen in a 3×3 grid and observed one sequence of this grid per each night. The field size of each grid point was $13'.6 \times 13'.6$ with a pixel scale of $0''.40$. Our program field, centered on the cluster, covers approximately $40' \times 40'$ which roughly corresponds to the area enclosed within the half tidal radius of ω Cen. Typical exposure times were 1400 s for Ca, 360 s for b, and 180 s for y, with the CCD being read out simultaneously through all four amplifiers, using an Arcon CCD controller. The observation log for the program fields is presented in Table 1. Two to four frames were taken in each band and each field.

The frames were calibrated from twilight or dawn sky flats and zero-level exposures, using the IRAF QUADPROC routines. Calibration frames were made by combining several individual exposures. All exposure times were sufficiently long that the center-to-corner shutter timing error was negligible. These procedures produced object frames with the sky flat to better than 1% in all filters. The IRAF routine COSMICRAYS was used to remove nearly all of the cosmic ray events in each frame, with conservative parameters set to avoid corrupting the stellar profiles.

Photometry of ω Cen stars was accomplished using DAOPHOT II and ALLSTAR (Stetson 1987, 1995). For each frame, a Moffat function PSF, varying cubically with radial position, was constructed using 100 to 200 bright, isolated, and unsaturated stars. The PSF was improved iteratively by subtracting faint nearby companions of the PSF stars. Aperture corrections were calculated using the program DAOGROW (Stetson 1990). The final aperture correction were made by adjusting the ALLSTAR magnitude of all stars by the weighted mean of the difference between the total aperture magnitude and the profile-fitting ALLSTAR magnitude for selected stars (e.g., PSF stars). After the aperture correction, we used DAOMATCH/DAOMASTER (Stetson 1992) to match stars of all frames covering the same field, and derived the average instrumental magnitude and colors on the same photometric scale. For each frame, the magnitude offset with respect to each master frame in Ca, b, and y was calculated, and photometry for the two to four frames for the same field was transformed to a common instrumental system.

On each night, five to seven standards from the list of Twarog & Anthony-Twarog (1995) were observed, and due to the small sample size the results for each night were combined. Comparison of the instrumental magnitudes for the final 15 observations in each filter with the standard values allowed the construction of linear transformations for the observed y, $b-y$, and hk magnitudes from the instrumental to the standard system. The standard stars observed cover a color range of 0.1 - 0.7 and 0.2 - 1.4 for $b-y$ and hk, respectively, and an air mass range of 1.0 - 1.6. Extinction

coefficients for all the filters were determined by a series of standard stars over a wide range of airmass. The final transformation equations were obtained by a linear least-square fit. They are

$$b - y = 0.956(b - y)_i - 0.013,$$

$$hk = 0.891hk_i - 1.013,$$

$$y = y_i + 0.026(b - y)_i - 5.007,$$

where $b - y$, hk, and y are the color indices and visual magnitude in the standard $Caby$ system, $(b - y)_i$, hk_i, and y_i refer to instrumental magnitudes corrected for extinction. No other trends in the residuals were noticeable, and therefore no additional terms in the transformation equations appear to be necessary. The calibration equations relate observed to standard values for y, $b - y$, and hk with standard deviations of 0.01, 0.01, and 0.02, respectively. During the observing runs, six field RR Lyrae "standard" stars (four RRab stars and two RRc stars) were observed in order to make a comparison between our result and that of B96, as discussed in the next section. Throughout, we have corrected for reddening using the reddening ratios, $E(b - y)/E(B - V) =$ 0.75, $E(hk)/E(b - y) =$ -0.1, adopted by B96.

3. METALLICITY CALIBRATION

B96 successfully provided the [Fe/H] vs. hk_o calibrations for two values of $(b - y)_o = 0.15$ and 0.30, from eight RRab stars and two RRc stars. Using these relations, it is possible to determine the metallicity of any RR Lyrae star for which there is $Caby$ photometry at either of these colors. However, in order to find the metallicity of RR Lyrae stars at arbitrary phase, it is necessary to find the relations between [Fe/H] and hk_o for various values of $(b - y)_o$ and ultimately produce a set of isometallicity lines that are continuous across the full range of $(b - y)_o$. In addition to two calibrations for $(b - y)_o = 0.15$ and 0.30, Baird & Anthony-Twarog (1999) added a new set of calibrations for a more complete grid of $(b - y)_o$ values [i.e., $(b - y)_o = 0.20$, 0.25, and 0.35] from high-quality photometric data for 14 RRab stars, combined with previous data from B96. As did B96, the metallicity values of Layden (1994) were adopted because they provide a uniform set of values for all the field RRab stars, and they are based on the Zinn & West (1984; hereafter ZW) metallicity scale for Galactic globular clusters. Layden's (1994) metallicities for RRab stars are based on the relative strengths of the Ca II K line and the H_δ, H_γ, and H_β Balmer lines. The [Fe/H] values of the RRc stars were adopted from Kemper (1982) and transformed to the ZW scale with Layden's (1994) equation. In the following discussion, we will denote $[Fe/H]_{spec}$ as the metallicity measured spectroscopically for RRab and RRc standard stars used in our calibration. The final $[Fe/H]_{hk}$ vs. hk_o relations were obtained by a straight line fit (Baird & Anthony-Twarog 1999). They are

$$[Fe/H]_{hk} = 8.11hk_o - 3.37\ (\sigma_{rms} = 0.110) \quad for\ \ (b - y)_o = 0.15,$$

$$[Fe/H]_{hk} = 7.75hk_o - 3.28\ (\sigma_{rms} = 0.055) \quad for\ \ (b - y)_o = 0.20,$$

$$[Fe/H]_{hk} = 7.45hk_o - 3.36\ (\sigma_{rms} = 0.035) \quad for\ \ (b-y)_o = 0.25,$$
$$[Fe/H]_{hk} = 6.44hk_o - 3.36\ (\sigma_{rms} = 0.040) \quad for\ \ (b-y)_o = 0.30,$$
$$[Fe/H]_{hk} = 5.06hk_o - 3.13\ (\sigma_{rms} = 0.074) \quad for\ \ (b-y)_o = 0.35.$$

The σ_{rms} are root mean square deviations calculated in the sense [Fe/H]$_{spec}$ - [Fe/H]$_{hk}$, where [Fe/H]$_{hk}$ is the value calculated from the observed hk_o values using the above relations. The σ_{rms} values are highest at the extreme colors, i.e., at $(b-y)_o = 0.15$ and 0.35, where the number of calibrating points is lowest.

Figure 1 shows the derived [Fe/H]$_{hk}$ vs. hk_o relations for five values of $(b-y)_o$, along with the photometric indices for 14 field RR Lyrae stars that define the relations. At warmer temperatures, the sensitivity of hk_o to [Fe/H]$_{hk}$ drops, and the slope in a [Fe/H]$_{hk}$ vs. hk_o relation becomes steeper. When stars get hotter than $(b-y)_o = 0.25$, the slopes of the [Fe/H]$_{hk}$ vs. hk_o relations are nearly the same, indicating that [Fe/H]$_{hk}$ is a function of hk_o only, as suggested by B96. $Caby$ photometry is useful for stars as blue as $(b-y)_o = 0.10$, but at higher temperatures the sensitivity of $Caby$ photometry to metallicity will certainly decrease, and the contamination by the H$_\epsilon$ line line should become quite substantial (Baird & Anthony-Twarog 1999).

We have calculated the metal abundance of the RR Lyrae stars in the field and ω Cen using the above [Fe/H]$_{hk}$ vs. hk_o relations. Additional [Fe/H]$_{hk}$ vs. hk_o relations were derived as necessary by interpolating these relations within the range of $0.15 < (b-y)_o < 0.35$. However, for stars with $(b-y)_o < 0.15$, which lie outside the limits of the current [Fe/H]$_{hk}$ vs. hk_o relations, we applied the relation for $(b-y)_o = 0.15$ because at these warm temperatures the isometallicity lines are horizontal in the $hk_o/(b-y)_o$ diagram, as described above. We estimate that, with these procedures, introduced uncertainties will be less than 0.1 dex at any point of the $hk_o/(b-y)_o$ diagram.

4. RESULTS

4.1. Field RR Lyrae Stars

To check the validity of our [Fe/H]$_{hk}$ calibration, we will compare our observations of field RR Lyraes with those by B96. Our measured values of [Fe/H]$_{hk}$ for field RR Lyrae stars are listed in Table 2, and comparison between spectroscopic metallicity, [Fe/H]$_{spec}$ (B96), and our [Fe/H]$_{hk}$ are shown in Figure 2. The [Fe/H]$_{spec}$ and the reddening of the stars was taken from Table 1 of B96. For the RRab stars, our [Fe/H]$_{hk}$ is in excellent agreement with [Fe/H]$_{spec}$, with an rms scatter of 0.12 dex. On the other hand, the [Fe/H]$_{hk}$ for the two RRc stars show larger scatter than that for the RRab stars. For V535 Mon, $(b-y)_o$ is very small, and the sensitivity of hk index is less than at redder colors, which might account for at least some of the discrepancy. The reason for the large deviation of AU Vir is not clear, however it anticipates the difficulties we have with the ΔS measurements for the ω Cen RRc stars, discussed below in sections 4.3 and 4.5.

Using the CTIO 4 m Telescope in 1997 December, Walker (1999) observed 14 *Caby* standard stars and three RR*ab* stars (U Lep, RY Col, HH Pup) from B96's list. We reduced this data in the same way as described above, and list the derived $[Fe/H]_{hk}$ for the RR Lyrae stars in Table 3. These stars are also plotted in Fig. 2, and are in excellent agreement both with our 0.9 m results and with $[Fe/H]_{spec}$. For all our RR*ab* stars and those of Walker (1999), the rms scatter of $[Fe/H]_{hk}$ corresponds to 0.10 dex.

4.2. ω Cen RR Lyrae Stars

In our program field of ω Cen, we measured 131 RR Lyrae stars, consisting of 74 RR*ab* and 57 RR*c* stars, which can be compared to the total of 180 ω Cen RR Lyrae stars known to date (Hogg 1973; Kaluzny et al. 1997b). For each RR Lyrae star we obtained two to four points of $b-y$ and hk, and dereddened using the reddening law stated in section 2. We adopted the reddening value $E(B-V) = 0.12$ from Harris (1996). BDE used $E(B-V) = 0.11$ which is essentially identical to the independent work of Dickens & Saunders (1965). Whitney et al. (1998) adopted $E(B-V) = 0.15$ for their analysis of the hot stellar population of the ω Cen. However, the effect of a small uncertainty in $E(B-V)$ values is negligible for our metallicity determination (Δ[Fe/H] < 0.02 dex). Additional correction for the interstellar contribution to the K line was ignored (Δ[Fe/H] $\sim$ 0.03 dex, see GTO). These both affect only the mean cluster [Fe/H] value, not the star-to-star scatter. Table 4 lists the dereddened values, $(b-y)_o$ and hk_o, and their photometric errors for each RR Lyrae star.

After obtaining the individual values of $[Fe/H]_{hk}$ for each RR Lyrae star, we calculated the mean value of the $[Fe/H]_{hk}$ by weighting with the photometric error of the hk value. A number of data points tagged as poor measurements were rejected, and some data points that showed a large deviation from their isometallicity line in the $hk_o/(b-y)_o$ diagram were also excluded. Table 5 lists our final weighted mean $[Fe/H]_{hk}$ values in column (3). Column (5) is the number of independent measurements used in the calculation of the mean $[Fe/H]_{hk}$. For the error of the mean $[Fe/H]_{hk}$ value, we adopted the standard deviation of the mean of the individual $[Fe/H]_{hk}$ measures. This error is listed as $\sigma_{[Fe/H]}$ in the column (4). For stars with only one data point, their $\sigma_{[Fe/H]}$ values have been set to blank. The typical value of $\sigma_{[Fe/H]}$ corresponds to about 0.20 dex. For those stars where the scatter is larger than typical, it is not clear whether this is due to observational error, or to some small non-repeatability and/or phase dependence in the $hk_o/(b-y)_o$ diagram as suggested by B96. We do not have sufficient observations per star to clarify this, and encourage more observations of the field "standard stars".[2] As a reference, we

[2] During the rapid rise to maximum of RR*ab* stars, one may question whether the effect of the sequence of exposure times for *Ca*, *b*, and *y* over more than half an hour will cause errors in the metallicity determinations. However, for a few identified data points on the rising branch, we did not find severe deviations from other data points in the $hk_o/(b-y)_o$ diagram. Furthermore, since our $[Fe/H]_{hk}$ corresponds to the mean of the individual measures and the

estimate the typical values of frame-to-frame scatter of HB stars as 0.02 and 0.03 mag for $b-y$ and hk, respectively. This scatter of hk corresponds to an error of less than 0.20 dex in [Fe/H], at any $b-y$.

4.3. Comparison with Previous ΔS Observations

Among the 131 RR Lyrae stars in our ω Cen field, 56 stars are in common with the previous ΔS observations of BDE and GTO, and we make a comparison between these values, $[Fe/H]_{\Delta S}$ [column (6) of Table 5], and those from our *Caby* photometry, $[Fe/H]_{hk}$ [column (3) of Table 5]. Most values of $[Fe/H]_{\Delta S}$ come from BDE, but for a few stars also observed by GTO, new values have been calculated by averaging the measurements of BDE and GTO. All $[Fe/H]_{\Delta S}$ values have been corrected to the ZW metallicity scale using the relation obtained by Layden (1994) (i.e., $[Fe/H]_{ZW} = 0.90[Fe/H]_{\Delta S}$ - 0.34) in order that all the [Fe/H] data is placed on a consistent metallicity scale. Figure 3 illustrates the residuals in the sense $[Fe/H]_{hk}$ - $[Fe/H]_{\Delta S}$ as a function of $[Fe/H]_{\Delta S}$. The closed circles are RR*ab* stars while open circles are RR*c* stars. The larger symbols represent stars with smaller observational error ($\sigma_{[Fe/H]} \leq 0.2$ dex) in $[Fe/H]_{hk}$. It is apparent that a significant difference between $[Fe/H]_{hk}$ and $[Fe/H]_{\Delta S}$ is present in a manner which is metallicity dependent.[3] The residuals for the RR*c* and RR*ab* stars appear similar, although the $[Fe/H]_{hk}$ for most RR*c* stars is metal-rich compared to $[Fe/H]_{\Delta S}$.

In order to more clearly see metallicity differences between $[Fe/H]_{hk}$ and $[Fe/H]_{\Delta S}$ in the $hk_o/(b-y)_o$ diagram, we introduce $hk_{o,\Delta S}$, which is the expected value of hk_o from $[Fe/H]_{\Delta S}$, and so construct a $hk_{o,\Delta S}/(b-y)_o$ diagram. We calculate $hk_{o,\Delta S}$ by inserting $[Fe/H]_{\Delta S}$ into inverse equations of our final [Fe/H] vs. hk_o relations. For the calculation of this $hk_{o,\Delta S}$, we retained our observed value of $(b-y)_o$. In Figure 4, we compare our observed $hk_o/(b-y)_o$ diagram with $hk_{o,\Delta S}/(b-y)_o$ for 56 RR Lyrae stars. In each diagram, we present schematic isometallicity lines, which were made from five [Fe/H] vs. hk_o relations with step size of 0.5 dex. It should be noted that our observed hk_o distribution for the RR*ab* stars is slightly more compressed than that of $hk_{o,\Delta S}$ for all $(b-y)_o$. In the case of the RR*c* stars and for some RR*ab* stars with $(b-y)_o < 0.2$, the distribution of hk_o is shifted in the metal-rich direction, by about 0.5 dex in the mean, compared to that of $hk_{o,\Delta S}$. These comparisons confirm that there are systematic differences between $[Fe/H]_{hk}$ and $[Fe/H]_{\Delta S}$.

---

typical error of the mean $[Fe/H]_{hk}$ value is small (about 0.2 dex), this effect should be negligible.

[3] Since Freeman & Rodgers (1975) used a bigger telescope, at higher dispersion, than did BDE, it is worth to make a comparison between our result and that of Freeman & Rodgers. However, we found the rms scatter between these two metallicities for 16 RR*ab* stars to be still large (0.37 dex).

4.4. Comparison with Other Metallicity Determinations

For 48 RR*ab* stars in ω Cen, Jurcsik (1998, hereafter J98) determined the empirical [Fe/H] values from the light-curve parameters using the observations of Kaluzny et al. (1997b). Comparing the empirical [Fe/H] values with the ΔS measurements of BDE and GTO samples for RR*ab* stars, J98 found significant discrepancies and suspected that the ΔS data of BDE and GTO were inaccurate. Schwarzenberg-Czerny & Kaluzny (1998; hereafter SK98) independently compared their empirical [Fe/H] with the ΔS metallicites, $[Fe/H]_{\Delta S}$, of BDE for 11 RR*ab* stars and revealed no obvious correlation between their empirical [Fe/H] and $[Fe/H]_{\Delta S}$. These results encouraged us to check for consistency between our $[Fe/H]_{hk}$ and the empirical [Fe/H] values of J98 and SK98.

Using the list of 47 RR*ab* stars employed by J98, we found the rms scatter between the metallicities of J98, $[Fe/H]_J$, and $[Fe/H]_{\Delta S}$ for 23 RR*ab* stars turned out to be large (0.48 dex), whereas that between $[Fe/H]_J$ and our $[Fe/H]_{hk}$ for 47 RR*ab* stars is much smaller (0.23 dex). Comparing the empirical metallicities independently obtained by SK98, $[Fe/H]_{SK98}$, with the ΔS observations for the 11 RR*ab* stars in common, significant discrepancies were found with a 0.44 dex rms scatter. However, from the comparison between $[Fe/H]_{SK98}$ and our $[Fe/H]_{hk}$ for 10 RR*ab* stars, the scatter reduced to 0.28 dex rms. In summary, both the empirical metallicities obtained from J98 and SK98 show larger deviation from $[Fe/H]_{\Delta S}$ of BDE and GTO than they do from from our photometric $[Fe/H]_{hk}$. Considering the assumed accuracy of the empirical metallicities as 0.10 - 0.15 dex (Jurcsik & Kovács 1996; J98 and references therein), this is strong evidence that the ΔS measurements of BDE and GTO are subject to larger errors than the authors state.

4.5. Metallicity Differences between $[Fe/H]_{hk}$ and $[Fe/H]_{\Delta S}$

What causes the systematic discrepancies between our $[Fe/H]_{hk}$ and the $[Fe/H]_{\Delta S}$ of BDE and GTO? We checked that there was no color dependency, which might be the case if our transformations as a function of color were incorrect. We also found that metallicity residuals between $[Fe/H]_{hk}$ and $[Fe/H]_{\Delta S}$ showed a similar pattern for the inner and outer regions of our program field, demonstrating that there is no dependency on image crowding.

We discuss supporting evidence for there being large errors in the ΔS measurements of BDE and GTO. First of all, the excellent agreement between $[Fe/H]_{hk}$ and $[Fe/H]_{spec}$, which is compatible to the ΔS measurements (see Layden 1994), of four field RR*ab* stars provides the most positive evidence of the accuracy of the present work and the large error of the ΔS results of BDE and GTO (see section 4.1). Second, there are non-negligible discrepancies between the results of BDE and GTO. GTO claimed that the internal errors are about 0.2 dex in both BDE and GTO ΔS measurements, and their system is thus not far from the standard ΔS system. However, as GTO already noted, a few stars (V32, V39, and V72) show large deviation (more than 0.5 dex) with BDE's results, probably, due to observation at phases far from the minimum

(see Fig. 2 of GTO). Furthermore, the rms scatter of the mean difference of the ΔS measurements between BDE and GTO corresponds to 0.34 dex, certainly not negligible. Third, J98 obtained an unexpectedly large (0.52 dex) rms scatter between her empirical metallicity values and ΔS metallicity of BDE, but comparing empirical data with GTO's observations, a smaller 0.38 dex rms scatter was obtained. Therefore, it is suspected that the ΔS measurements for ω Cen, especially BDE's data, are inaccurate. Both of the empirical metallicities obtained from J98 and SK98 show smaller rms scatter in our $[Fe/H]_{hk}$ than in ΔS metallicity, $[Fe/H]_{\Delta S}$ (see section 4.4). This suggests that our $[Fe/H]_{hk}$ are more accurate than the $[Fe/H]_{\Delta S}$ of BDE and GTO. Fourth, despite a more extensive sample than that of previous ΔS observations, the relation between magnitude and metallicity of our observations show a smaller scatter. We also note consistency with the model predictions of Lee (1991) (see section 5.1 and Fig. 6). Finally, as we will see in section 4.6, the metallicity distribution of our observations for RR*ab* stars is more consistent with that of the giant stars of Suntzeff & Kraft (1996, hereafter SK), rather than that of the previous ΔS observations. It was also suggested by SK that the large population of very metal-poor stars found from ΔS measurements is incorrect. According to stellar evolution theory, the RR Lyrae stars are an intrinsically abundance-biased population due to the low probability that the extremely metal-rich (-poor) red (blue) HB stars evolve through the instability strip (Lee & Demarque 1990). Therefore, it is unreasonable to expect that the metallicity distribution of RR Lyrae stars is wider than that of their progenitor stars. Consequently, we conclude that the systematic discrepancies between our $[Fe/H]_{hk}$ and the $[Fe/H]_{\Delta S}$ of BDE and GTO are caused by the large uncertainties of the ΔS measurements.

Finally, we discuss the difference in metallicity distribution in our results between the RR*ab* and RR*c* stars. Our distribution of metal-rich RR*c* stars is difficult to understand from the standpoint of standard metal-rich HB evolutionary tracks, which do not penetrate into the hotter regions of the instability strip (Lee & Demarque 1990). While no definite resolution on the disagreement in the metallicity can be offered, we suggest that the metal enhancement of RR*c* stars may be due to the possible contamination of Ca II H by H_ϵ. For hotter stars, inclusion of the H_ϵ feature will weaken the metallicity effect because the weakening of the Ca II H line can be partially compensated by the growth of the Balmer line (Anthony-Twarog et al. 1991). Although we used the [Fe/H] vs. hk_o relation at $(b-y)_o = 0.15$ for stars with $(b-y)_o < 0.15$ (see section 3), we should treat this data with caution until the [Fe/H] vs. hk_o relations at higher temperatures are confirmed. Furthermore, because the [Fe/H] vs. hk_o relation at high temperature [e.g., $(b-y)_o = 0.15$], as shown in Fig. 1, does not extend to metallicity higher than [Fe/H] = -1.0, the metal-rich end of the RR*c* stars may also be suspect. More calibration data for RR*c* stars will be needed to resolve this problem. For this reason, we regard our results for RR*c* stars to be tentative, and we will restrict our analysis to RR*ab* stars in the following discussions.

4.6. The Metallicity Distribution

Considering the homogeneity and large sample size of the present database, it is worthwhile to investigate the metallicity distribution of RR Lyrae stars and compare it with the earlier results for RR Lyrae stars and giant stars (BDE; Dickens 1989; Norris et al. 1996; SK). However, care must be taken when comparing the metallicity distribution of RR Lyrae stars and giant stars, since as mentioned above RR Lyrae stars are intrinsically an abundance-biased sample due to the failure of the extremely metal-rich red HB stars to penetrate into the instability strip. Furthermore, the frequency of RR Lyrae stars at a given metallicity depends on the HB morphology as well as the metallicity distribution of the underlying stellar population (e.g., Lee 1992 and Walker & Terndrup 1991 for RR Lyrae stars in Baade's window). Figure 5 presents the metallicity distributions for the RR*ab* stars and giant stars. All of the earlier studies and our results agree on the non-Gaussian shape of the metallicity distribution which contains a sharp rise from the low metallicity side, a modal value of [Fe/H] $\approx$ -1.8 and a tail of metal-rich stars reaching at least [Fe/H] $\approx$ -0.9. For the 161 - star bright giant (BG) sample and the 199 - star subgiant (SGB) sample of SK (Fig. 5c), the metallicity distribution is narrower than that of 34 - star RR*ab* sample obtained from the ΔS method (Fig. 5a). SK suggested that the large population of very metal-poor stars found in the ΔS measurement is due to the large rms error of 0.4 dex of the old ΔS study and probably the strong low-metallicity tail of the error distribution is spurious. The more complete sample of RR*ab* stars from our *hk* method (Fig. 5b) also shows the paucity of very metal-poor stars. Consequently, contrary to the case of the ΔS observations, the range of the metallicity distribution of our observations for RR*ab* stars is consistent with that of the giant stars of SK.

While a detailed discussion of the origin of the abundance distribution is outside the scope of this paper, we wish to point out that in the analysis of a B, V CMD for ω Cen containing 130,000 stars, Lee et al. (1999) found several distinct red giant branches (RGBs). They also showed from population models that the most metal-rich RGB is about 2 Gyr younger than the dominant metal-poor component, suggesting that ω Cen has enriched itself over this timescale. An extensive study of the metallicity distribution for an homogeneous and nearly complete sample of ω Cen giant branch stars, now underway, will place this result on a firmer footing. The RR Lyrae stars, being clearly representatives of the oldest populations in ω Cen, will be an important part of any enrichment model for the cluster.

5. DISCUSSION

5.1. The M_V(RR) - [Fe/H] Relation

Given our homogeneous metallicity measurements for nearly the whole sample of ω Cen RR Lyrae stars, we can turn to a discussion of the magnitude-metallicity relation. We will use the intensity mean magnitude values, $< V >$, given in BDE and Kaluzny et al. (1997b). For the stars

whose $< V >$ values are available from both sources the mean values have been adopted. Column (7) of Table 5 lists the $< V >$ for each RR Lyrae stars. While the photometry of BDE is restricted to the outer region of the cluster, that of Kaluzny et al. (1997b) covers a larger area including the central region from their extensive observations (Kaluzny et al. 1996, 1997a). Although Kaluzny et al. (1997b) have claimed field-to-field differences on the level of a few hundredth's of magnitude and uncertainties when combining photometry obtained in different fields for the same variables, we adopted the averaged value of magnitude for stars with multiple entries in their Table 1. From intercomparison of 66 RR Lyrae stars between BDE and Kaluzny et al. (1997b), we found a zeropoint offset of $< V >$ as -0.03 $\pm$ 0.06 in the sense BDE minus Kaluzny et al. (1997b). However, considering the intrinsic spread (or scatter) and random error of $< V >$ for ω Cen RR Lyrae stars, this small offset would have only a small or negligible effect on the discussion of the M_V(RR) - [Fe/H] relation. We are presently reducing BV photometry for ω Cen RR Lyrae stars, which in the future will provide a more homogeneous and consistent dataset of $< V >$.

Using the data in Table 5, the observed correlation between M_V(RR) and [Fe/H] is presented in Figure 6, where panel (a) is based on [Fe/H] determined by the previous ΔS measurements while panel (b) is based on our new *Caby* photometry. In the transformation to the absolute magnitude, we adopted a distance modulus of V - M_V = 14.1 based on the recent evolutionary models of M_V(RR) by Demarque et al. (1999). In Fig. 6b, closed circles are stars which overlap with the sample of BDE and GTO (i.e., Fig. 6a), while triangles represent stars only observed in our study. The large symbols are for stars with smaller observational error ($\sigma_{[Fe/H]} \leq 0.2$ dex) of the $[Fe/H]_{hk}$ with the same criterion of Fig. 3. It appears that the random errors of $[Fe/H]_{hk}$ are smaller than those of $[Fe/H]_{\Delta S}$ in the M_V(RR) - [Fe/H] distribution. In particular, V5 ($[Fe/H]_{\Delta S}$ = -2.32) and V56 ($[Fe/H]_{\Delta S}$ = -1.82), which are fainter (about 0.2 mag.) than similarly metal-poor RR Lyrae stars in the M_V(RR) - $[Fe/H]_{\Delta S}$ diagram, are moved to relatively metal-rich $[Fe/H]_{hk}$. Their new metallicities ($[Fe/H]_{hk}$ = -1.35 and -1.26) are more consistent with their intrinsic luminosity, following a general trend shown in Fig. 6b.

We have superimposed the model correlations of Lee (1991), which were constructed based on his HB population models under two assumptions regarding the variation of HB type with metallicity. The solid (age = 13.5 Gyr) and short-dashed (age = 15.0 Gyr) lines are for the case that the HB type follows the nonmonotonic behavior with decreasing [Fe/H] similar to that observed in the Galactic globular cluster system [see Fig. 3 of Lee (1991)]. Lee (1991) suggested that this nonmonotonic behavior of HB morphology is perhaps due either to the highly nonlinear relationship between mass loss and [Fe/H] or to some combination of the effects of mass loss and enhanced α-elements, although the complete understanding is still lacking. The long-dashed line is a simple model locus, with fixed mass loss, age, and α-elements, which fails to reproduce the observed nonmonotonic behavior of HB type with decreasing [Fe/H]. The sudden upturn in M_V(RR) of model loci can be explained by a series of HB population models (see Fig. 5 of Lee 1993), where one can see how sensitively the population of the instability strip changes with decreasing [Fe/H]. As [Fe/H] decreases, there is a certain point where the zero age portion of the

HB just crosses the blue edge of the instability strip. Then, only highly evolved stars from the blue HB can penetrate back into the instability strip, and the mean RR Lyrae luminosity increases abruptly (Lee 1993). As shown in Fig. 6b, the correlation predicted from the model loci, including the sudden upturn in M_V(RR), agree better with our new M_V(RR) - $[Fe/H]_{hk}$ distribution. Note that the choice of HB evolutionary tracks has little effect on this conclusion, as Demarque et al. (1999) recently showed that new synthetic HB models based on evolutionary tracks with improved input physics (Yi et al. 1997) produce qualitatively the same results.

Lee (1991) noted that the solid line in the M_V(RR) - $[Fe/H]_{\Delta S}$ diagram of Fig. 6a does not pass through a few stars at $[Fe/H]_{\Delta S} \approx$ -1.4, and he suspected this deviation is perhaps due either to the observational errors or to the zero point uncertainty of the metallicity scale. Alternatively, he suggested that a better match is obtained by the older model locus of 15.0 Gyr (i.e., short-dashed line of Fig. 6). In our new diagram of Fig. 6b, we can see that these deviant stars are now moved to $[Fe/H]_{hk} \approx$ -1.5 and are, therefore, more well matched to the model locus. With our new data, the best match with the models is expected somewhere between the solid and dashed lines (i.e., $\sim$ 14.3 Gyr). Note that the absolute ages in these models are based on the assumption that the mean age of the inner halo clusters is $\sim$ 14.5 Gyr, thus this result suggests ω Cen is comparable in age with other inner halo clusters.

If we remove stars in the range -1.9 < $[Fe/H]_{hk}$ < -1.5, where most of the variables are believed to be extremely evolved stars (see section 5.4 below), then we obtain $\Delta M_V(RR)/\Delta[Fe/H] = 0.24 \pm 0.04$, which is consistent, to within the errors, with the slopes obtained by LDZ and Lee (1990) from the evolutionary models, excluding the clusters in this metallicity range. Consequently, RR Lyrae stars in ω Cen and their nonlinear M_V(RR) - [Fe/H] relations from our observations provide a strong support for the LDZ and Lee (1990) evolutionary models. This non-linearity, which also implies that the relation between period-shift and metallicity is not linear (see section 5.3 below), would clarify some of the disagreements with other investigators because fits of straight lines to different data sets produce significantly different slopes.

5.2. The m_{bol} - logT_{eff} Diagram of RR Lyrae Stars

In order to test more clearly the metallicity dependence of the luminosity of RR Lyrae stars, we constructed the bolometric magnitude (m_{bol}) - temperature (T_{eff}) diagram for RR*ab* stars of different metallicities in Figure 7. Panel (a) and (b) contains 27 and 34 RR*ab* stars for which [Fe/H] has been determined from the ΔS method and our *Caby* photometry, respectively. For the $B-V$, we used the equilibrium color defined by Bingham et al. (1984), $(B-V)_{eq} = \frac{2}{3} < B-V > + \frac{1}{3}(< B > - < V >)$. In the calculations of T_{eff} and bolometric correction, we adopted a color-temperature relation that has been used in the construction of the Revised Yale Isochrones (Green et al. 1987; see Green 1988) for the consistency with the work of Lee (1991). The color information, $< B-V >$ and $< B > - < V >$, of the ω Cen variables was taken from Sandage (1981).

Fig. 7a shows that the relationship between metallicity and bolometric magnitude is not clear when the metallicities determined by previous ΔS observations are used (Dickens 1989). Not all the faintest stars are the most metal-rich stars, and some metal-rich stars are apparently as bright as the metal-poor stars. On the other hand, as shown in Fig 7b, the metallicity dependence of RR Lyrae magnitude becomes more distinct when we use our new $[Fe/H]_{hk}$ metallicities. Now, most metal-rich RR Lyrae stars lie below (i.e., having fainter magnitude) the RR Lyrae stars that are relatively more metal-poor. The cases of V5 and V56 were discussed above in this context. The magnitude gap between the metal-rich and metal-poor RR Lyrae stars near $m_{bol} \approx 14.6$ is due to the abrupt increase, in magnitude at approximately [Fe/H] = -1.5 (see Fig. 6b).

5.3. The Period Shift Effect

If the relationship between M_V(RR) and $[Fe/H]_{hk}$ is not linear as noticed above, we expect a similar correlation between period-shift and [Fe/H] for ω Cen RR Lyrae stars. In order to confirm this, we obtained the period-shifts of ω Cen RR*ab* stars at a fixed T_{eff} from the deviations in the period of each ω Cen RR*ab* star from the M3 fiducial line in the logP - logT_{eff} plane. Periods have been obtained mainly from Kaluzny et al. (1997b), but for some stars we adopted the values of BDE. Column (8) of Table 5 gives the period for each RR Lyrae star. As we did in section 5.2, we also used the $(B-V)_{eq}$, calculated from the photometry of Sandage (1981) and $(B-V)$ - T_{eff} relations of Green et al. (1987) in the calculations of T_{eff} for M3 RR Lyrae stars. We transformed the observed periods of M3 RR*c* stars to fundamental periods by adding 0.125 to their logarithms (Bingham et al. 1984; LDZ) to obtain the logP - logT_{eff} relationship for all the M3 RR Lyraes.

The correlation between period-shift, $\Delta \log P(T_{eff})$, and [Fe/H] is shown in Figure 8. Assuming no large differences between P′ and P even in the case of M_{bol} range ($\sim$ 0.2 mag) for ω Cen RR Lyrae stars, we superimposed the model loci of ΔlogP′(T_{eff}) - [Fe/H] of Lee (1993; see his Fig. 6b) for the comparison with observations. The P′ corresponds to the "reduced period", which is corrected for the differing luminosity within the cluster by normalizing to the mean magnitude of RR Lyrae stars (see LDZ). As shown in Fig. 8a, for the 27 RR*ab* stars, whose [Fe/H] has been determined by the ΔS method, there is no distinct ΔlogP(T_{eff}) - $[Fe/H]_{\Delta S}$ correlation. It should be noted that the period-shift values for metal-rich stars show similar or even larger shifts, compared to metal-poor stars. This metallicity effect of the period-shift is much smaller than that found in the period-shift - [Fe/H] relationship of Oosterhoff I and Oosterhoff II clusters, as well as the field RR Lyrae stars covering a similar range of metallicity (LDZ; Lee 1990, 1993). However, when we adopt our new metallicity, $[Fe/H]_{hk}$, a more clear correlation between ΔlogP(T_{eff}) and $[Fe/H]_{hk}$ emerges (Fig. 8b) which follows the model locus of Lee (1993), despite some scatter among the metal-poor stars. This is expected, ω Cen RR Lyrae stars should show more scatter than the models for globular cluster system because post-ZAHB luminosity evolution causes scatter in period-shifts and also because only single determinations of period and [Fe/H] exists for individual ω Cen RR Lyrae stars, whereas those for the clusters represent averages over many stars

(see Lee 1990). As in the M_V(RR) - $[Fe/H]_{hk}$ diagram, V5 and V56 now belong to the metal-rich stars in ΔlogP(T_{eff}) - $[Fe/H]_{hk}$ diagram. The RR Lyrae stars having -1.9 < [Fe/H] < -1.5, which are considered to be highly evolved stars arisen from the bluest HBs, are shifted in period relative to M3 variables of the same T_{eff} by approximately the same (or even larger) amounts as the variables in the more metal-poor RR Lyrae stars (see section 5.4 below). Consequently, our new correlation between period-shift and $[Fe/H]_{hk}$ shows roughly the same trend as the M_V(RR) - $[Fe/H]_{hk}$ relation, and is more in agreement with the model locus.

5.4. Highly Evolved RR Lyrae Stars

The effect of post ZAHB evolution plays a key role in our understanding of the M_V(RR) - [Fe/H] relation and other related problems, such as the Sandage period-shift effect (see also Lee 1993 and references therein). In particular, the evolutionary models of Lee (1990) suggest that the RR Lyrae stars in very blue HB clusters within the range -2.0<[Fe/H]<-1.6 are highly evolved stars from the bluest HBs, and have significantly brighter magnitudes and longer periods than those near the ZAHB (see also Figs. 6 and 8). Highly evolved RR Lyrae stars can be identified from a star's position in a period (logP) - blue amplitude (A_B) diagram by comparing them with RR Lyrae stars in clusters having similar metallicity but with redder HB morphology (Jones et al. 1992; Cacciari et al. 1992; Clement & Shelton 1999). Assuming that A_B depends on [Fe/H] as well as T_{eff} (LDZ; Caputo 1988), at a fixed metallicity, relative A_B values are reliable indicators of relative T_{eff}. Therefore, highly evolved RR Lyrae stars in ω Cen can be detected from a series of logP - A_B diagrams covering the range of metallicities.

Figure 9 shows a logP - A_B diagram for ω Cen RR*ab* stars at three metallicity groups with $[Fe/H]_{hk}$ < -1.9, -1.9 ≤ $[Fe/H]_{hk}$ < -1.5, and $[Fe/H]_{hk}$ ≥ -1.5, respectively. The A_B values are from Sandage (1981) as given in column (9) of Table 5. For comparison, we also plotted RR*ab* stars in M15 ([Fe/H] = -2.17; Lee, Demarque, & Zinn 1994), M3 ([Fe/H] = -1.66), and M4 ([Fe/H] = -1.28) for each metallicity group, respectively, with data from Sandage (1990b). The solid line represents the fiducial line of the lower envelope to the M3 distribution of logP - A_B (Sandage 1990a). For the most metal-poor (Fig. 9a) and the most metal-rich stars (Fig. 9c), the majority of ω Cen RR Lyrae stars do not, respectively, show deviations from the M15 and M4 variables. This would indicate that the evolutionary stages of these ω Cen variables are not significantly different from those for variables in M15 and M4, respectively. However, most ω Cen RR*ab* stars in the range -1.9 ≤ [Fe/H] < -1.5 are obviously deviant when compared to the M3 variables. These stars have much longer periods than M3 variables of similar A_B, thus most of them are probably evolved with higher luminosities. In order to provide a reference for highly evolved stars, in Fig. 9b, we include two field RR*ab* stars, SU Dra and SS Leo (open triangles), which have similar metallicity to M3, but are considered to be in a highly evolved and luminous state (Jones et al. 1992). The open square represents a M3 RR*ab* star (V65), which is in a more advanced evolutionary state than the majority of M3 RR*ab* stars (Kaluzny et al. 1998; Clement & Shelton 1999). Kaluzny et

al. (1998) noted two other highly evolved M3 RR*ab* stars, V14 and V104. The similarity of all of these stars to those in ω Cen confirms that most ω Cen RR*ab* stars in the range -1.9 $\leq$ [Fe/H] $<$ -1.5 are in a highly evolved stage of their HB evolution.

Recently, Clement & Shelton (1999) re-examined the logP - V amplitude (A_V) relation of RR Lyrae stars in globular clusters of both Oosterhoff types by applying the test of Jurcsik & Kovács (1996) to identify and remove Blazhko variables. They concluded that the logP - A_V relation for "normal" RR*ab* stars is not a function of metal abundance, but rather, related to the Oosterhoff type. Along with the discovery of three bright M3 RR*ab* stars in a more advanced evolutionary state, they also concluded that the Oosterhoff dichotomy has something to do with evolution off the ZAHB. This is consistent with our result presented here, and these observations provide a support to the LDZ hypothesis that evolution away from the ZAHB plays a crucial role in the Oosterhoff period dichotomy (see also Lee & Carney 1999).

6. SUMMARY AND CONCLUSIONS

We present new metallicity measurements of 131 RR Lyrae stars in the ω Cen using the hk index of the $Caby$ photometric system. From our study, we draw the following conclusions:

(1) We provide the most complete and homogeneous metallicity data to date, with a typical internal error of 0.20 dex, based on the [Fe/H] vs. hk_o calibrations of Baird & Anthony-Twarog (1999).

(2) For RR Lyrae stars in common with the ΔS observations of BDE and GTO, we find that our metallicity values, $[Fe/H]_{hk}$, are systematically deviant from the ΔS metallicities, $[Fe/H]_{\Delta S}$, whereas the $[Fe/H]_{hk}$ for well observed field RR*ab* stars are consistent with previous spectroscopic measurements. With some supporting evidence, we find that this discrepancy is due to errors in the BDE and GTO results.

(3) The M_V(RR) - [Fe/H] and period-shift - [Fe/H] relations from our observations show a tight distribution with a nearly step function change in luminosity near [Fe/H] = -1.5. This is consistent with the model predictions of Lee (1991), which suggest that the luminosity of RR Lyrae stars depends on evolutionary status as well as metallicity.

(4) From a series of logP - A_B diagrams at a range of metallicities, we also identify highly evolved RR*ab* stars in the range of -1.9 $\leq$ $[Fe/H]_{hk}$ $<$ -1.5, as predicted from the synthetic HB models. Therefore, this gives support to LDZ's hypothesis that evolution away from the ZAHB plays a role in the Oosterhoff dichotomy.

Some work remains to be done in the future. As noted already, because the [Fe/H] vs. hk_o relation at high temperature [e.g., $(b-y)_o = 0.15$] shown in Fig. 1 does not extend to metallicities higher than [Fe/H] = -1.0, the metal-rich calibration for the RR*c* stars may be suspect. More calibration data are needed to resolve this problem. Furthermore, more RR*c* stars should be observed to check whether there is any difference between the RR*ab* and RR*c* calibrations. Additionally, in order to test the viability of the field RR Lyrae stars calibration, it would be

valuable to observe samples of RR Lyrae stars in a number of globular clusters with various and well-determined metallicities. Then we can determine if the calibrations for field RR Lyrae stars are consistent with those for the globular cluster RR Lyrae stars. On the theoretical side, it would be useful to study the relationship between [Fe/H] and *hk* using synthetic spectra, and in particular, clarify the problem of the contamination of Ca II H by Hϵ for hotter stars. Finally, with its distinct advantages such as ease of observations and analysis, the *hk* method should supersede the old ΔS method in determining the metallicity of RR Lyrae stars, despite the need for more accurate calibrations.

We would like to thank A. Jurcsik and N. Suntzeff for providing electronic copies of their datasets, and an anonymous referee for a careful review and useful comments. S.-C.R. is grateful to Suk-Jin Yoon for his helpful efforts in some model calculations. Support for this work was provided by the Creative Research Initiatives Program of Korean Ministry of Science & Technology, and in part by the Korea Science & Engineering Foundation through grant 95-0702-01-01-3.

A. NOTES ON INDIVIDUAL RR LYRAE STARS

*V*24.−V24 ([Fe/H]$_{hk}$ = -1.86) has a very small period-shift value [ΔlogP(T$_{eff}$) = -0.09], compared with normal RR*ab* stars (see Fig. 8b). Considering its light-curve characteristics, such as period (0.4623 day; Kaluzny et al. 1997b) and blue amplitude (A$_B$ = 0.47; Sandage 1981) (see Fig. 9b), and sinusoidal light-curve shape (Kaluzny et al. 1997b), V24 is likely to be an RR*c* star.

*V*52.−Kaluzny et al. (1997b) suggested that V52, which is the brightest RR*ab* star ($< V >$ = 13.95), is actually a BL Her variable. However, its period (0.66 day) is significantly shorter than the 0.75 day, short period limit found for Pop. II Cepheids (Wallerstein & Cox 1984).

*V*7, *V*116, *and V*149.−Unlike other metal-rich stars, V116 and V149 show brighter magnitudes, comparable to those of relatively metal-poor stars (see Fig. 6b). Considering the large deviation in the logP - A$_B$ diagram (see Fig. 9), V149 is probably a highly evolved RR Lyrae star. According to its period (0.72 day) and V amplitude, A$_V$ (0.54 mag, Kaluzny et al. 1997b), V116 is likely to be in a similar evolutionary state. Although the luminosity is not as high as that of V116 and V149, considering its large deviation in the logP - A$_B$ diagram and metallicity ([Fe/H]$_{hk}$ = -1.46) close to the boundary for the evolved stars, it is not unreasonable to consider V7 as a highly evolved star, also.

REFERENCES

Anthony-Twarog, B. J., Laird, J. N., Payne, D., & Twarog, B. A. 1991, AJ, 101, 1902

Anthony-Twarog, B. J., & Twarog, B. A. 1998, AJ, 116, 1922

Baird, S. R. 1996, AJ, 112, 2132 (B96)

Baird, S. R., & Anthony-Twarog, B. J. 1999, in preparation

Bingham, E. A., Cacciari, C., Dickens, R. J., & Fusi Pecci, F. 1984, MNRAS, 209, 765

Butler, D., Dickens, R. J., & Epps, E. A. 1978, ApJ, 225, 148 (BDE)

Cacciari, C., Clementini, G., & Fernley, J. A. 1992, ApJ, 396, 219

Caputo, F. 1988, A&A, 189, 70

Clement, C. M., & Shelton, I. 1999, ApJ, 515, L85

Demarque, P., Zinn, R., Lee, Y.-W., & Yi, S. 2000, AJ, in press

Dickens, R. J. 1989, in IAU Colloq. 111, The Use of Pulsating Stars in Fundamental Problems of Astronomy, ed. E. G. Schmidt (Cambridge: Cambridge Univ. Press), p. 141

Dickens, R. J., & Saunders, J. 1965, R. Obs. Bull., No. 101

Freeman, K. C., & Rodgers, A. W. 1975, ApJ, 201, L71

Gratton, R.G., Tornambe, A., & Ortolani, S. 1986, A&A, 169, 111 (GTO)

Green, E. M. 1988, in Calibration of Stellar Ages, ed. A. G. D. Philip (Schenectady: Davis), p. 81

Green, E. M., Demarque, P., & King, C. R. 1987, The Revised Yale Isochrones and Luminosity Functions (New Haven: Yale Univ. Observatory)

Harris, W. E. 1996, AJ, 112, 1487

Hogg, H. S. 1973, Publ. David Dunlop Obs., 3, No. 6

Jones, R. V., Carney, B. W., Storm, J., & Latham, W. 1992, ApJ, 386, 646

Jurcsik, J. 1998, ApJ, 506, L113 (J98)

Jurcsik, J., & Kovács, G. 1996, A&A, 312, 111

Kaluzny, J., Hilditch, R., Clement, C., & Rucinski, S. M. 1998, MNRAS, 296, 347

Kaluzny, J., Kubiak, M., Szymanski, M., Udalski, A., Krzeminski, W., & Mateo, M. 1996, A&AS, 120, 139

Kaluzny, J., Kubiak, M., Szymanski, M., Udalski, A., Krzeminski, W., Mateo, M., & Stanek, K. 1997a, A&AS, 122, 471

Kaluzny, J., Kubiak, M., Szymanski, M., Udalski, A., Krzeminski, W., & Mateo, M. 1997b, A&AS, 125, 343

Kemper, E. 1982, AJ, 87, 1395

Layden, A. C. 1994, AJ, 108, 1016

Layden, A. C., Hanson, R. B., Hawley, S. L., Klemola, A. R., & Hanley, C. J. 1996, AJ, 112, 2110

Lee, J.-W., & Carney, B. W. 1999, AJ, 118, 1373

Lee, Y.-W. 1990, ApJ, 363, 159

Lee, Y.-W. 1991, ApJ, 373, L43

Lee, Y.-W. 1992, AJ, 104, 1780

Lee, Y.-W. 1993, in IAU Colloq. 139, New Perspectives on Stellar Pulsation and Pulsating Variable Stars, ed. J. Nemec and D. Welch (Cambridge: Cambridge Univ. Press), p. 294.

Lee, Y.-W., & Demarque, P. 1990, ApJS, 73, 709

Lee, Y.-W., Demarque, P., & Zinn, R. 1990, ApJ, 350, 155 (LDZ)

Lee, Y.-W., Demarque, P., & Zinn, R. 1994, ApJ, 423, 248

Lee, Y.-W., Joo, J.-M., Sohn, Y.-J., Rey, S.-C., Lee, H.-c., & Walker, A. R. 1999, Nature, 402, 55

Norris, J. E., Freeman, K. C., & Mighell, K. J. 1996, ApJ, 462, 241

Sandage, A. 1981, ApJ, 248, 161

Sandage, A. 1982, ApJ, 252, 553

Sandage, A. 1990a, ApJ, 350, 603

Sandage, A. 1990b, ApJ, 350, 631

Schwarzenberg-Czerny, A., & Kaluzny. J. 1998, MNRAS, 300, 251 (SK98)

Smith, H. A. 1995, RR Lyrae Stars (Cambridge: Cambridge Univ. Press)

Stetson, P. B. 1987, PASP, 99, 191

Stetson, P. B. 1990, PASP, 102, 932

Stetson, P. B. 1992, in IAU Colloq. 136, Stellar Photometry-Current Techniques and Future Developments, ed. C. J. Butler and I. Elliot (Cambridge: Cambridge Univ. Press), p. 291

Stetson, P. B. 1995, DAOPHOT II User's Manual (Victoria: Dominian Astrophys. Obs.)

Suntzeff, N. B., & Kraft, R. P. 1996, AJ, 111, 1913 (SK)

Twarog, B. A., & Anthony-Twarog, B. J. 1991, AJ, 101, 237

Twarog, B. A., & Anthony-Twarog, B. J. 1995, AJ, 109, 2828

Zinn, R., & West, M. J. 1984, ApJS, 55, 45 (ZW)

Walker, A. R. 1999, in preparation

Walker, A. R., & Terndrup, D. M. 1991, ApJ, 378, 119

Wallerstein, G., & Cox, A. N. 1984, PASP, 96, 677

Whitney, J. H., Rood, R. T., O'Connell, R. W., D'Cruz, N. L., Dorman, B., Landsman, W. B., Bohlin, R. C., Roberts, M. S., Smith, A. M., & Stecher, T. P. 1998, ApJ, 495, 284

Yi, S., Demarque, P., & Kim, Y.-C. 1997, ApJ, 482, 677

This preprint was prepared with the AAS LaTeX macros v4.0.

Table 1. ω Cen Observation Log

			Exposures (number×seconds)			
Observing Date	Field	Frame Center (arcmin)	y	b	Ca	FWHM (arcsec)
27/28 March 1997	F1	18 SE	1×180	1×360	1×1200	1.9
	F2	13 E	1×180	1×360	1×1400	1.8
	F3	18 NE	1×180	1×360	1×1400	1.7
	F4	13 N	1×180	1×360	1×1400	1.8
	F5	cluster center	1×180	1×360	1×1400	1.6
	F6	13 S	1×180	1×360	1×1400	1.5
	F7	18 SW	1×180	1×360	1×1400	1.6
	F8	13 W	1×180	1×360	1×1400	1.6
	F9	18 NW	1×180	1×360	1×1400	1.5
28/29 March 1997	F1	18 SE	1×180	1×360	1×1400	2.1
	F2	13 E	1×180	1×360	1×1400	2.2
	F3	18 NE	1×180	1×360	1×1400	2.0
	F4	13 N	1×180	1×360	1×1400	1.8
	F5	cluster center	1×180	1×360	1×1400	1.8
	F6	13 S	1×180	1×360	1×1400	2.0
	F7	18 SW	1×180	1×360	1×1400	1.9
	F8	13 W	1×180	1×360	1×1400	2.0
	F9	18 NW	1×180	1×360	1×1400	1.9
29/30 March 1997	F1	18 SE	1×180	1×360	1×1400	1.7
	F2	13 E	2×180	2×360	2×1400	1.6
	F3	18 NE	1×180	1×360	1×1400	1.6
	F4	13 N	...	...	...	...
	F5	cluster center	1×180	1×360	1×1400	1.6
	F6	13 S	1×180	1×360	1×1400	1.6
	F7	18 SW	1×180	1×360	1×1400	1.6
	F8	13 W	1×180	1×360	1×1400	1.5
	F9	18 NW	1×180	1×360	1×1400	1.7

Table 2. Observations of Field RR Lyrae Stars

Star	$E(B-V)^a$	$(b-y)_o$	hk_o	$[Fe/H]_{spec}{}^a$	$[Fe/H]_{hk}$	Type
WY Ant	0.014	0.334	0.274	-1.66	-1.71	ab
RY Col	0.012	0.304	0.339	-1.11	-1.18	ab
U Lep	0.014	0.326	0.247	-1.93	-1.83	ab
HH Pup	0.060	0.229	0.369	-0.69	-0.52	ab
V535 Mon	0.113	0.039	0.141	-1.64	-2.23	c
AU Vir	0.005	0.169	0.307	-2.00	-0.90	c

[a] From Baird (1996)

Table 3. Observations of Field RR Lyrae Stars with CTIO 4 m Telescope

Star	$E(B-V)^a$	$(b-y)_o$	hk_o	$[Fe/H]_{spec}{}^a$	$[Fe/H]_{hk}$	Type
RY Col	0.012	0.296	0.357	-1.11	-1.06	ab
U Lep	0.014	0.241	0.205	-1.93	-1.83	ab
HH Pup	0.060	0.293	0.386	-0.69	-0.77	ab

[a] From Baird (1996)

Table 4. Photometric Data for ω Cen RR Lyrae Stars*

	data1				data2				data3				
Variable	$(b-y)_o$	σ_{b-y}	hk_o	σ_{hk}	$(b-y)_o$	σ_{b-y}	hk_o	σ_{hk}	$(b-y)_o$	σ_{b-y}	hk_o	σ_{hk}	(
3	0.257	0.010	0.244	0.009	0.255	0.020	0.239	0.018	0.189	0.029	0.235	0.026	
4	0.303	0.009	0.259	0.009	0.301	0.010	0.245	0.010	···	···	···	···	
5	0.283	0.008	0.312	0.010	0.243	0.008	0.260	0.010	···	···	···	···	
7	0.315	0.010	0.290	0.012	0.230	0.010	0.255	0.011	···	···	···	···	
8	0.291	0.011	0.262	0.014	0.323	0.012	0.190	0.013	···	···	···	···	
9	0.268	0.016	0.262	0.012	0.307	0.015	0.292	0.016	0.319	0.031	0.282	0.029	
10	0.174	0.010	0.196	0.010	0.236	0.010	0.229	0.009	···	···	···	···	
11	0.301	0.011	0.244	0.010	0.098	0.007	0.220	0.006	0.277	0.010	0.220	0.012	
12	0.149	0.008	0.236	0.009	0.163	0.009	0.237	0.009	0.247	0.009	0.216	0.011	
13	0.322	0.025	0.234	0.030	···	···	···	···	···	···	···	···	
14	0.140	0.007	0.213	0.008	0.178	0.009	0.183	0.012	···	···	···	···	
15	0.319	0.010	0.285	0.011	0.223	0.009	0.274	0.010	0.322	0.009	0.188	0.010	
16	0.154	0.007	0.262	0.007	0.156	0.008	0.241	0.012	0.150	0.010	0.256	0.011	
18	0.308	0.010	0.254	0.010	0.273	0.009	0.272	0.010	0.272	0.012	0.161	0.012	
19	0.215	0.012	0.268	0.011	0.128	0.011	0.266	0.011	0.196	0.010	0.274	0.013	
21	0.084	0.009	0.317	0.008	0.161	0.008	0.290	0.009	···	···	···	···	
22	0.240	0.013	0.230	0.012	0.212	0.009	0.241	0.011	0.192	0.011	0.179	0.012	
23	0.301	0.013	0.363	0.014	0.289	0.015	0.349	0.013	0.304	0.013	0.317	0.019	
24	0.206	0.013	0.185	0.012	0.215	0.010	0.185	0.015	0.207	0.012	0.186	0.014	
25	0.146	0.012	0.236	0.014	0.275	0.017	0.265	0.016	0.287	0.019	0.235	0.017	

*Table 4 is presented in its complete form in the electronic edition of the Astronomical Journal.
A portion is shown here for guidance regarding its form and content.

Table 5. Metallicities and Photometric Parameters for ω Cen RR Lyrae Stars

Variable	Type	$[Fe/H]_{hk}$	$\sigma_{[Fe/H]}$	N	$[Fe/H]_{\Delta S}{}^{a}$	$< V >^{b}$	Period (days)^{b}	$A_B{}^{c}$
3	ab	-1.54	0.05	3	-1.35	14.39	0.8413	0.92
4	ab	-1.74	0.05	2	-1.65	14.50	0.6273	1.29
5	ab	-1.35	0.08	2	-2.32	14.75	0.5154	1.28
7	ab	-1.46	0.08	2	-1.84	14.53	0.7130	1.13
8	ab	-1.91	0.28	2	-1.91	14.65	0.5213	1.39
9	ab	-1.49	0.06	3	-1.01	14.78	0.5235	0.97
10	c	-1.66	0.10	2	-1.82	14.51	0.3750	0.52
11	ab	-1.67	0.13	3	···	14.55	0.5645	···
12	c	-1.53	0.14	3	···	14.54	0.3868	···
13	ab	-1.91	···	1	-1.72	14.48	0.6691	1.14
14	c	-1.71	0.13	2	-2.22	14.55	0.3771	0.61
15	ab	-1.64	0.39	3	···	14.41	0.8107	···
16	c	-1.29	0.08	3	···	14.56	0.3302	0.57
18	ab	-1.78	0.28	4	-2.01	14.52	0.6217	1.29
19	c	-1.22	0.05	3	···	14.86	0.2996	0.54
21	c	-0.90	0.11	2	···	14.41	0.3808	···
22	c	-1.63	0.17	4	-2.35	14.54	0.3960	0.54
23	ab	-1.08	0.14	3	···	14.83	0.5109	···
24	ab	-1.86	0.03	3	···	14.45	0.4623	0.47
25	c	-1.57	0.14	3	···	14.50	0.5885	···
26	ab	-1.68	0.10	3	···	14.50	0.7846	···
27	ab	-1.50	0.26	3	-1.38	14.75	0.6157	0.69
30	c	-1.75	0.17	3	···	14.49	0.4039	···
32	ab	-1.53	0.16	2	-1.55	14.48	0.6204	1.33
33	ab	-2.09	0.23	3	-2.02	14.54	0.6023	1.36
34	ab	-1.71	···	1	-1.44	14.49	0.7340	0.95
35	c	-1.56	0.08	4	···	14.56	0.3868	···
36	c	-1.49	0.23	2	-2.02	14.52	0.3798	0.55
38	ab	-1.75	0.18	3	-1.85	14.52	0.7791	0.75
39	c	-1.96	0.29	4	-1.98	14.57	0.3934	0.56
40	ab	-1.60	0.08	3	···	14.53	0.6341	···
41	ab	-1.89	0.48	2	···	14.50	0.6630	···
44	ab	-1.40	0.12	3	-1.12	14.70	0.5675	1.12
45	ab	-1.78	0.25	3	-1.44	14.53	0.5891	1.25
46	ab	-1.88	0.17	3	···	14.49	0.6870	1.14
47	c	-1.58	0.31	3	···	14.29	0.4851	0.46

Table 5—Continued

Variable	Type	$[Fe/H]_{hk}$	$\sigma_{[Fe/H]}$	N	$[Fe/H]_{\Delta S}{}^{a}$	$< V >^{b}$	Period (days)^{b}	$A_B{}^{c}$
49	ab	-1.98	0.11	2	-2.08	14.63	0.6046	1.12
50	c	-1.59	0.19	3	···	14.64	0.3862	0.53
51	ab	-1.64	0.21	3	···	14.53	0.5742	···
52	ab	-1.42	0.04	3	···	13.95	0.6604	···
54	ab	-1.66	0.12	2	···	14.42	0.7729	0.83
55	ab	-1.23	0.31	3	-1.14	14.77	0.5817	1.01
56	ab	-1.26	0.15	3	-1.82	14.75	0.5680	1.01
57	ab	-1.89	0.14	3	-1.96	14.48	0.7946	0.75
58	c	-1.37	0.18	3	···	14.52	0.3699	0.25
59	ab	-1.00	0.28	2	···	14.76	0.5185	···
62	ab	-1.62	0.29	3	···	14.48	0.6199	···
63	ab	-1.73	0.09	3	-2.12	14.50	0.8259	0.57
64	c	-1.46	0.23	4	-1.63	14.56	0.3446	0.57
66	c	-1.68	0.34	4	···	14.58	0.4075	···
67	ab	-1.10	···	1	-1.04	14.69	0.5644	1.10
68	c	-1.60	0.01	2	-1.95	14.25	0.5346	0.52
69	ab	-1.52	0.14	2	-1.91	14.56	0.6532	1.15
70	c	-1.94	0.15	3	···	14.53	0.3907	0.49
72	c	-1.32	0.22	3	-1.88	14.54	0.3845	0.52
73	ab	-1.50	0.09	3	···	14.52	0.5752	1.31
74	ab	-1.83	0.36	2	-1.82	14.59	0.5032	1.49
75	c	-1.49	0.08	2	···	14.47	0.4221	0.45
76	c	-1.45	0.13	2	-2.09	14.57	0.3380	0.42
77	c	-1.81	···	1	-1.68	14.53	0.4263	0.48
79	ab	-1.39	0.18	4	-1.60	14.61	0.6083	1.30
81	c	-1.72	0.31	3	···	14.56	0.3894	0.52
82	c	-1.56	0.20	4	···	14.51	0.3358	0.53
83	c	-1.30	0.22	2	-1.76	14.59	0.3566	0.57
84	c	-1.47	0.10	3	-0.80	14.28	0.5799	0.81
85	ab	-1.87	0.31	3	-1.38	14.48	0.7427	0.86
86	ab	-1.81	0.18	3	···	14.54	0.6479	···
87	c	-1.44	0.19	3	···	14.60	0.3965	···
88	ab	-1.65	0.23	3	···	14.23	0.6904	···
89	c	-1.37	0.28	3	-1.38	14.57	0.3749	···
90	ab	-2.21	···	1	···	14.53	0.6034	···
91	ab	-1.44	0.17	2	···	···	···	···

Table 5—Continued

Variable	Type	$[Fe/H]_{hk}$	$\sigma_{[Fe/H]}$	N	$[Fe/H]_{\Delta S}{}^{a}$	$< V >^{b}$	Period (days)^{b}	$A_B{}^{c}$
94	c	-1.00	0.11	2	···	14.76	0.2539	0.31
95	c	-1.84	0.55	3	-1.57	14.52	0.4050	0.49
96	ab	-1.22	···	1	-1.49	···	0.6245	0.89
97	ab	-1.56	0.37	3	···	14.53	0.6919	···
98	c	-1.05	0.12	2	···	14.84	0.2806	···
99	ab	-1.66	0.14	3	-1.28	14.30	0.7661	1.13
100	ab	-1.58	0.14	3	···	···	···	···
101	c	-1.88	0.32	4	···	14.72	0.3410	0.44
102	ab	-1.84	0.13	4	···	14.55	0.6914	···
103	c	-1.92	0.11	3	···	···	···	···
104	ab	-1.83	0.18	4	-1.79	14.48	0.8663	0.41
105	c	-1.24	0.18	4	···	14.70	0.3353	0.55
106	ab	-1.50	0.23	3	···	···	···	···
107	ab	-1.36	0.11	2	···	14.82	0.5141	···
108	ab	-1.93	0.23	2	···	14.62	0.5945	···
109	ab	-1.51	0.25	3	···	14.45	0.7439	···
110	c	-2.14	0.16	3	···	···	···	···
111	ab	-1.66	0.04	2	···	14.46	0.7630	···
112	ab	-1.81	0.26	3	···	14.60	0.4743	···
113	ab	-1.65	0.34	3	···	14.60	0.5733	···
114	ab	-1.32	0.30	3	-2.12	···	···	0.75
115	ab	-1.87	0.01	2	···	14.55	0.6305	1.18
116	ab	-1.27	0.44	2	···	14.27	0.7200	···
117	c	-1.68	0.25	3	···	14.50	0.4216	···
118	ab	-1.62	0.23	3	-1.80	14.43	0.6116	···
119	c	-1.61	0.10	3	-1.22	14.66	0.3059	···
120	ab	-1.39	0.06	3	···	14.74	0.5486	···
121	c	-1.46	0.13	3	···	14.58	0.3042	···
122	ab	-2.02	0.18	3	···	14.52	0.6349	···
123	c	-1.64	0.01	2	···	14.48	0.4743	0.49
124	c	-1.33	0.23	3	-1.65	14.60	0.3319	0.60
125	ab	-1.67	0.22	3	-0.99	14.59	0.5929	1.42
126	c	-1.31	0.13	3	-1.96	14.59	0.3420	0.52
127	c	-1.59	0.08	2	···	14.62	0.3053	0.38
128	ab	-1.88	0.04	2	···	14.32	0.8350	···
130	ab	-1.46	0.17	2	···	14.70	0.4932	1.10

Table 5—Continued

Variable	Type	$[Fe/H]_{hk}$	$\sigma_{[Fe/H]}$	N	$[Fe/H]_{\Delta S}$[a]	$< V >$[b]	Period (days)[b]	A_B[c]
131	c	-1.56	0.20	3	···	14.50	0.3921	···
132	ab	-1.91	0.20	3	···	···	···	···
134	ab	-1.80	0.41	3	-1.83	14.52	0.6529	1.27
135	ab	-2.20	···	1	···	···	···	···
136	c	-1.83	0.47	3	-2.12	···	···	···
137	c	-1.19	0.18	3	···	14.53	0.3342	···
139	ab	-1.46	0.04	3	-2.01	14.35	0.6768	···
141	ab	-1.55	0.36	2	···	···	···	···
143	ab	-1.87	0.14	3	···	···	···	···
144	ab	-1.71	0.12	3	-1.38	14.41	0.8352	···
145	c	-1.58	0.07	3	-2.12	14.56	0.3732	···
147	c	-1.66	0.14	3	···	···	···	···
149	ab	-1.21	0.24	3	···	14.42	0.6827	1.21
150	ab	-1.76	0.34	3	···	···	···	···
151	c	-1.30	0.24	3	···	14.55	0.4078	0.42
153	c	-1.38	0.19	3	-1.60	14.55	0.3863	···
154	c	-1.39	0.12	3	···	···	···	···
155	c	-1.46	0.09	3	···	14.50	0.4139	···
156	c	-1.40	0.04	2	···	···	···	···
157	c	-1.49	0.10	3	···	14.56	0.4066	···
158	c	-1.25	0.06	2	···	14.59	0.3673	···
160	c	-1.66	···	1	-2.01	14.55	0.3973	0.52
163	c	-1.18	0.27	3	-2.07	14.56	0.3132	0.27

[a] From Butler et al. (1978) and Gratton et al. (1986).

[b] From Butler et al. (1978) and Kaluzny et al. (1997b).

[c] From Sandage (1981).

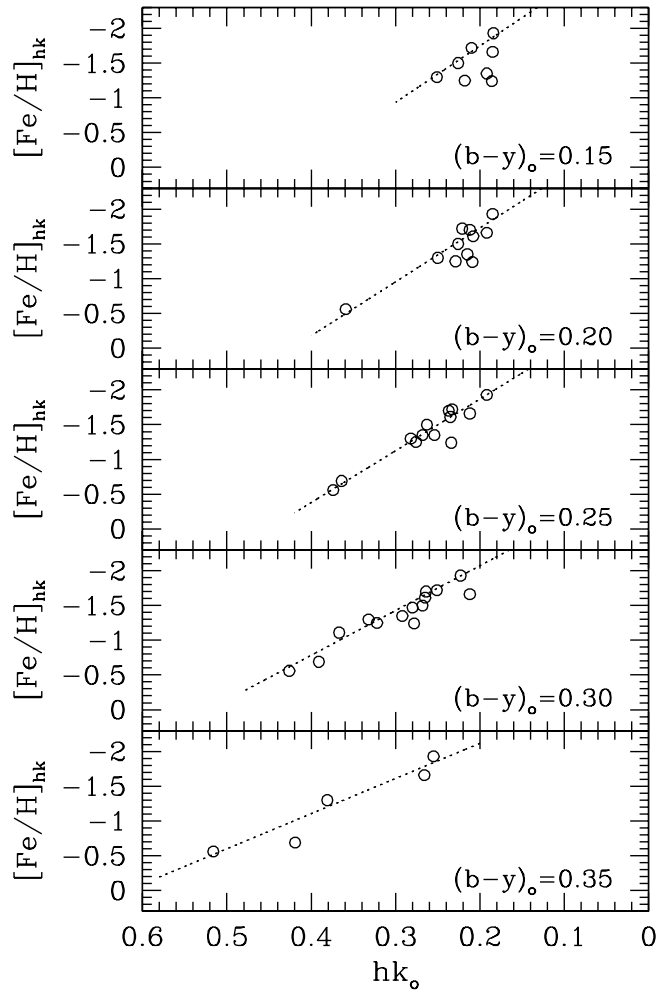

Fig. 1.— The relations between the metallicity measured from our hk index, [Fe/H]$_{hk}$, and hk_o at $(b-y)_o$ = 0.15, 0.20, 0.25, 0.30, and 0.35 (Baird & Anthony-Twarog 1999). As temperature increases the sensitivity of hk_o to [Fe/H]$_{hk}$ drops.

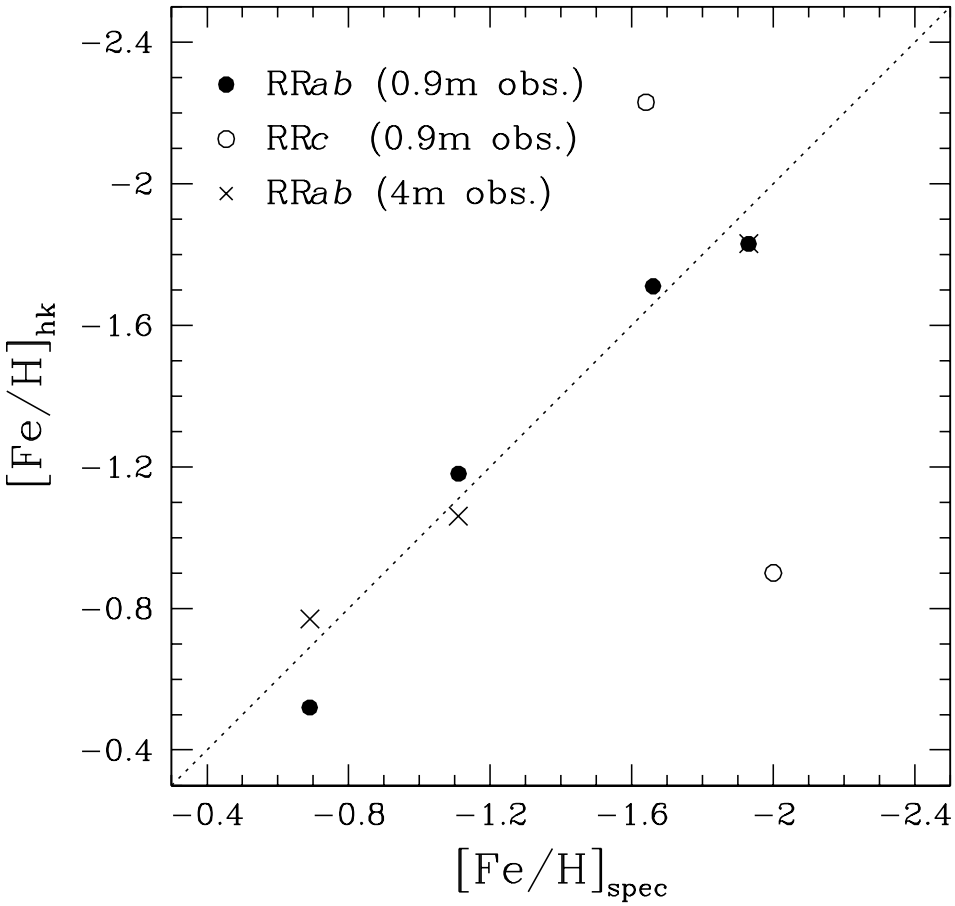

Fig. 2.— Comparison between the metallicity measured spectroscopically, $[Fe/H]_{spec}$ (Baird 1996), and that from our *hk* index, $[Fe/H]_{hk}$, for field RR Lyrae stars. The $[Fe/H]_{hk}$ for the RR*ab* stars are in excellent agreement with $[Fe/H]_{spec}$, but two RR*c* stars show a larger scatter.

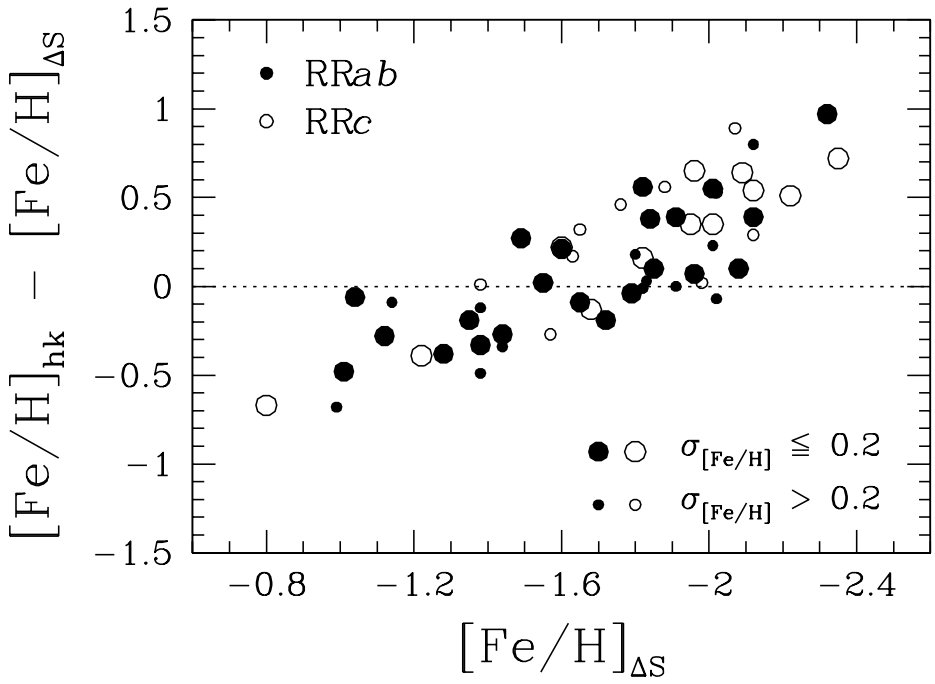

Fig. 3.— Comparison between the metallicity measured from our hk index, [Fe/H]$_{hk}$, and that from previous ΔS observations, [Fe/H]$_{\Delta S}$, for 56 ω Cen RR Lyrae stars. The larger symbols are for stars with smaller ($\sigma_{[Fe/H]} \leq 0.2$ dex) observational error in [Fe/H]$_{hk}$. Note the significant differences between [Fe/H]$_{hk}$ and [Fe/H]$_{\Delta S}$.

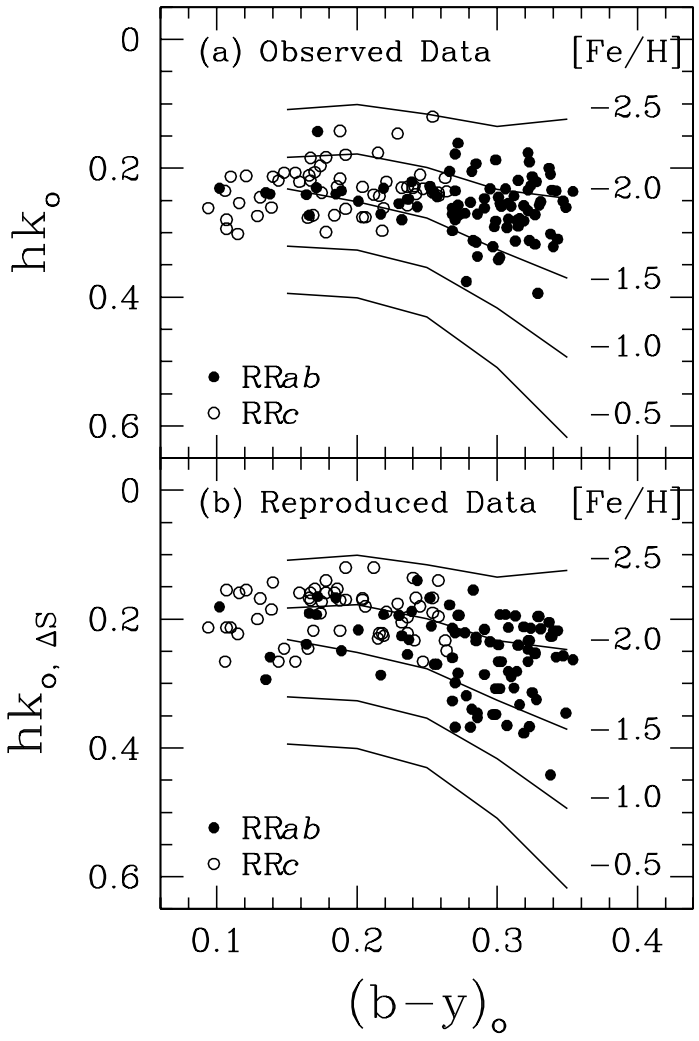

Fig. 4.— Comparison between (a) observed $hk_o/(b-y)_o$ diagram and (b) reproduced $hk_{o,\Delta S}/(b-y)_o$ diagram. Note that our observed hk_o distribution of RRab stars is more compressed than that of $hk_{o,\Delta S}$, which is the expected value from the $[\mathrm{Fe/H}]_{\Delta S}$, at any fixed $(b-y)_o$. In the case of most RRc stars and some RRab stars with $(b-y)_o < 0.2$, the distribution of hk_o is shifted more metal rich (about 0.5 dex) in the mean, compared to that of $hk_{o,\Delta S}$ (see text).

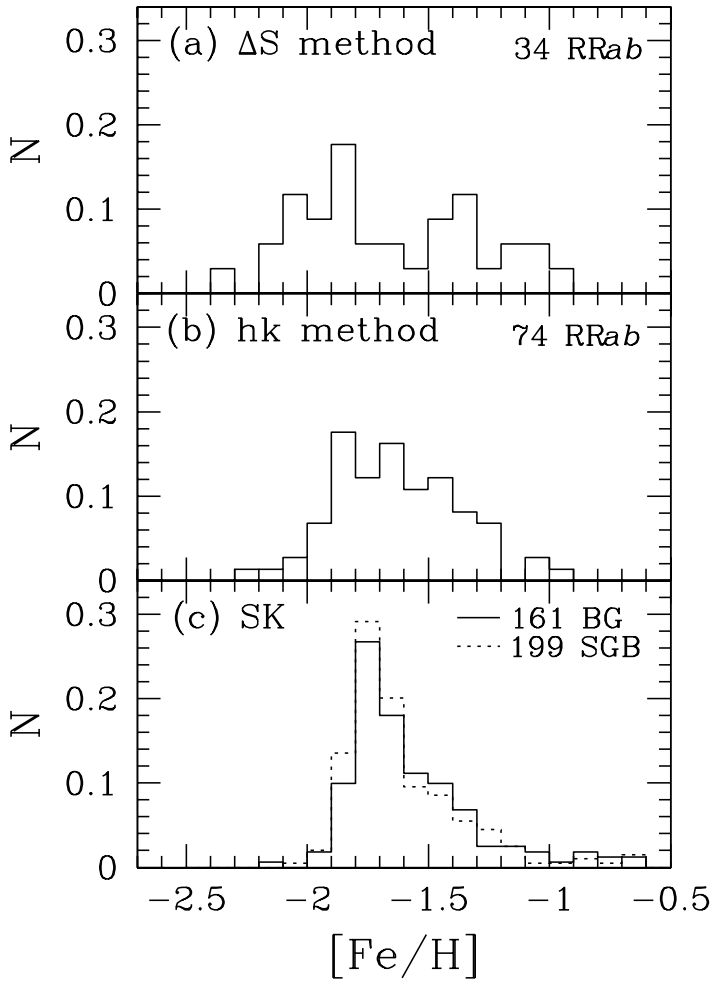

Fig. 5.— The metallicity distributions for (a) 34 RR*ab* stars obtained from the ΔS measurements, (b) our 74 RR*ab* stars obtained from the *hk* method, and (c) 161 bright giants (BG; solid line) and 199 subgiants (SGB; dotted line) from Suntzeff & Kraft (1996). All metallicities are on the Zinn & West (1984) scale.

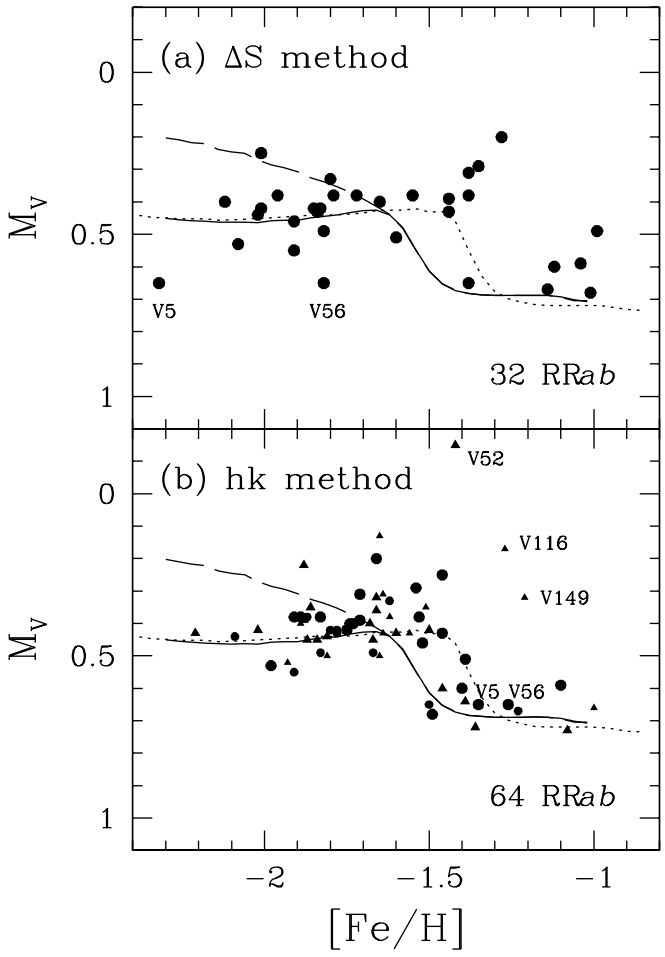

Fig. 6.— The M_V(RR) - [Fe/H] relation of RR Lyrae stars in ω Cen based on (a) the metallicity data for 32 RR*ab* stars obtained from the ΔS method, and (b) the metallicity data for 64 RR*ab* stars from our *hk* method. The closed circles are stars overlapping with the sample of the ΔS measurements, while the closed triangles are stars available only from our photometry. The long-dashed line is a simple model locus of Lee (1991) for the ensemble average of the RR Lyrae luminosities within the instability strip with fixed mass loss, age, and α-elements. The solid (age = 13.5 Gyr) and short-dashed (age = 15.0 Gyr) lines are model loci which include the nonmonotonic behavior of the horizontal-branch type with decreasing [Fe/H]. The M_V(RR) - $[Fe/H]_{hk}$ distribution appears to be in excellent agreement with the model loci (see text).

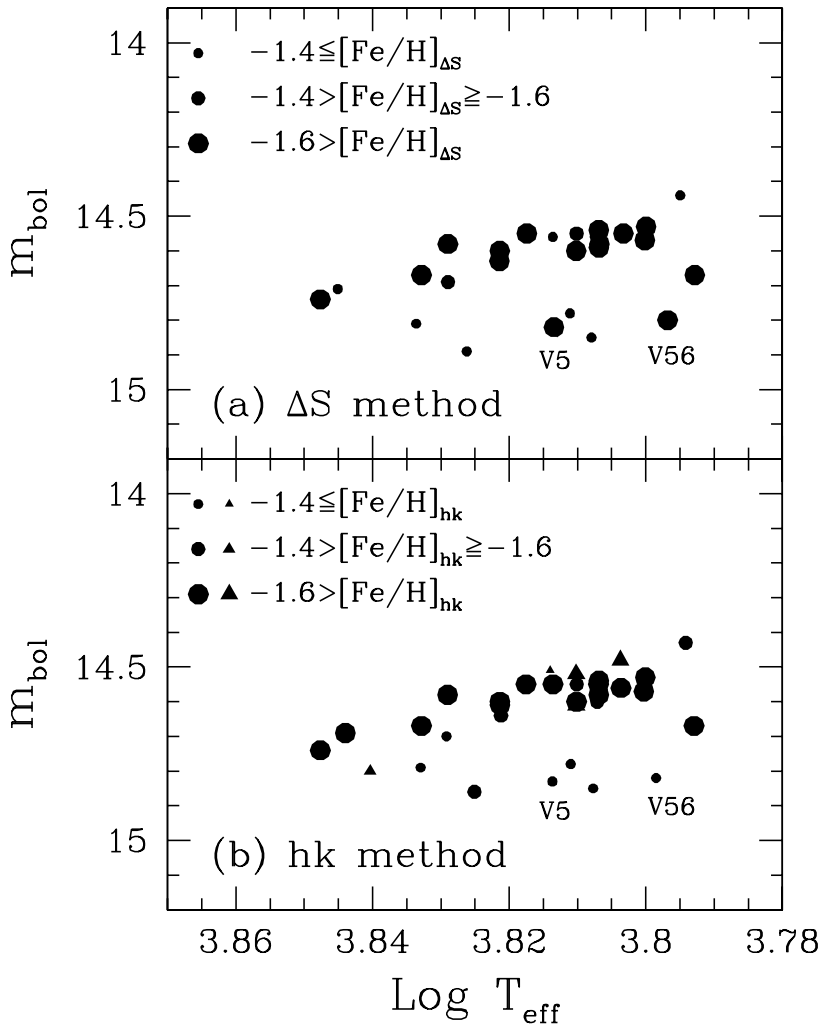

Fig. 7.— (a) The m_{bol} - $\log T_{eff}$ diagram for 27 RR*ab* stars in ω Cen, with metallicity data obtained from the ΔS method. There is no clear relationship between metallicity and bolometric magnitude. (b) Same as (a) for 34 RR*ab* stars with metallicity data obtained from our *hk* method. The closed circles are stars overlapping with the sample of the ΔS measurement, while the closed triangles are variables only available from our photometry. Note that the metallicity dependence of m_{bol} is more clearly defined in (b).

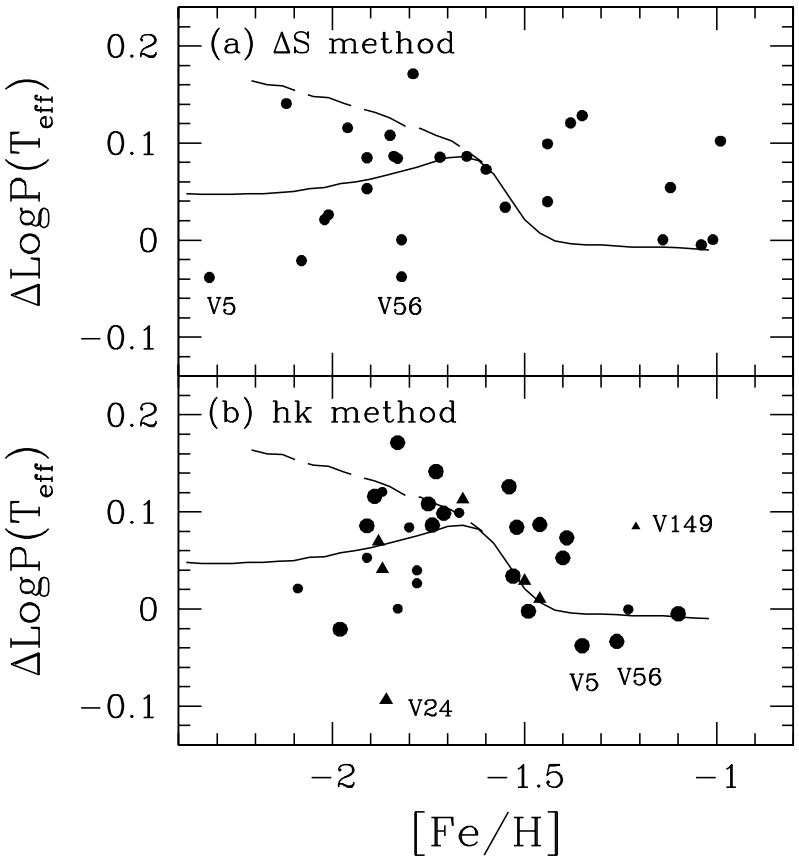

Fig. 8.— (a) The $\Delta \log P(T_{eff})$ - [Fe/H] diagram for 27 RR*ab* stars in ω Cen, with metallicity data obtained from the ΔS method. As in Fig. 6, the solid and long dashed lines are model loci from Lee (1993). (b) Same as (a) for 34 RR*ab* stars with metallicity data obtained from our *hk* method. The closed triangles represent variables only available from our photometry. Note again that our new observations agree better with the model predictions.

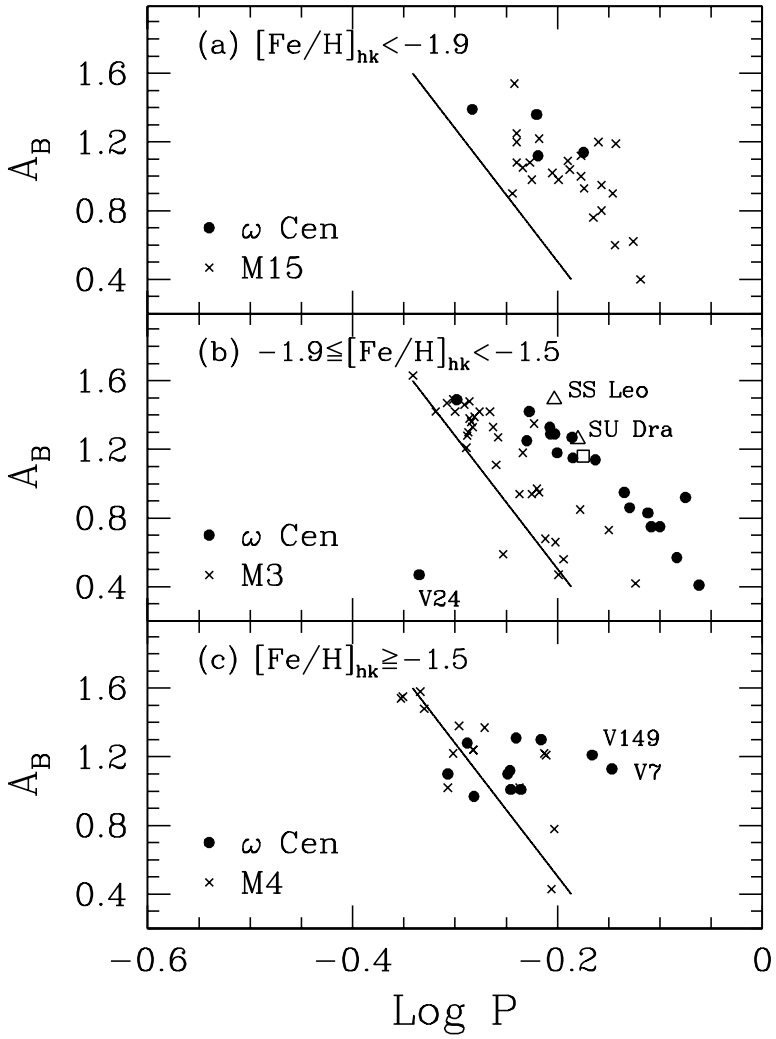

Fig. 9.— (a) LogP-A_B diagram for RR*ab* stars with [Fe/H]$_{hk}$ < -1.9. The solid line is a fiducial line corresponding to the lower envelope of the M3 distribution, from Sandage (1990a). (b) Same as (a) for stars with -1.9 ≤ [Fe/H]$_{hk}$ < -1.5. We include two highly evolved field RR*ab* stars, SU Dra and SS Leo (open triangles), from Jones et al. (1992). A highly evolved RR*ab* star in M3, V65, is also marked with an open square (Clement & Shelton 1999). Most of ω Cen RR*ab* stars in this metallicity range are believed to be highly evolved because they show an obvious deviation from M3 variables. (c) Same as (a) for stars with [Fe/H]$_{hk}$ ≥ -1.5.